A New Chemorheological Analysis of Highly Filled Thermosets Used in Integrated Circuit Packaging

PETER J. HALLEY

Department of Chemical Engineering, The University of Queensland, Brisbane QLD 4072, Australia

Received 6 March 1996; accepted 24 June 1996

ABSTRACT: Chemorheology (and thus process modeling) of highly filled thermosets used in integrated circuit (IC) packaging has been complicated by their highly filled nature, fast kinetics of curing, and viscoelastic nature. This article summarizes a more thorough chemorheological analysis of a typical IC packaging thermoset material, including novel isothermal and nonisothermal multiwave parallel-plate chemorheology. This new chemorheological analysis may be used to optimize existing and design new IC packaging processes. © 1997 John Wiley & Sons, Inc. J Appl Polym Sci **64:** 95–106, 1997

Key words: Chemorheology; thermosets; chemoviscosity; gelation; epoxy

INTRODUCTION

Traditionally design, operation, and optimization of integrated circuit (IC) packaging has been undertaken by empirical trial and error methods, due to the complexity of the flow and gelation behavior (chemorheology) of the highly filled thermoset encapsulants. However, these trial-and-error methods inevitably lead to high design and raw material costs. Clearly, a more scientific model of the IC packaging process that incorporates an understanding of the complex chemorheology of these materials is required.

Highly filled thermoset materials (typically epoxy-molding compounds) are used in IC packaging due to their low cost (high silica loading), high thermal conductivity and low thermal expansion, which enables good integration with other chip components. However, these materials show highly complex chemorheological (chemoviscosity and gelation) behavior due to their highly filled nature, fast kinetics of curing, and viscoelastic nature. Recent work on the rheology of highly filled thermosets is scarce; however, Nguyen[1,2] investigated the use of nonisothermal dynamic parallel-plate rheometry to characterize the chemorheology of highly filled thermoset IC packaging material and used these data to produce realistic flow simulations. However, it is noted that measurements are made using individual dynamic shear rate tests, which may be influenced by sample-to-sample variation. Also, the correlation between dynamic viscosity and steady shear viscosity is assumed to follow the modified Cox–Merz rule[3] but it has not been checked. Peters et al.[4] also investigated nonisothermal dynamic parallel-plate rheometry to describe the chemorheology of highly filled thermoset IC packaging materials, but required flow visualization measurements to refine chemorheological data for model development. Once again, the potential sample-to-sample variability and dynamic-steady viscosity assumptions were present. Pahl and Hesenkamp[5] investigated isothermal parallel-plate rheometry to characterize the chemorheology of moderately filled epoxy-molding compounds for use in the development of a chemorheological model and compared this model with nonisothermal data. However, data were obtained from dynamic rate sweeps, which are prone to unwanted effects of cure due to the experimental time required at each frequency. Interestingly, Pahl and Hesenkamp showed that the original Cox–Merz rule[6] applies. Previous work by Halley et al.[7] showed

Contract grant sponsors: Moldflow; The University of Queensland

that the use of multiwave tests (developed by Holly et al.[8]) using simultaneous multiple-frequency signals alleviates the effect of experimentation time on the gelation of unfilled TGDDM/DDS resin systems. Ng and Manas-Zloczower[9] quantified the effects of filler loading on the gelation of highly filled epoxy-molding compounds by isothermal dynamic parallel-plate rheometry.

Studies into the chemorheology of filled thermoset systems were also made at high shear rates. Blyler et al.[10] used a capillary rheometer inside a transfer mold to measure the isothermal and nonisothermal flow characteristics of filled epoxy-molding compounds. Cure effects, however, were not considered. Han and Wang[11] developed a modified slit rheometer with a reservoir attachment to characterize the chemoviscosity of filled epoxy-molding compounds. They were able to characterize the viscosity of the materials as a function of shear rate, temperature, and cure (by controlling time in the reservoir). However, cure sampling was cumbersome and gelation times were not monitored. Manzione and Weld[12] developed a flow visualization method for IC packaging to verify existing flow simulation models, but did not explicitly calculate chemoviscosity model parameters. Gonzalez et al.[13] used a numerical parameter identification scheme to determine chemoviscosity model parameters from the minimization between the difference of simulation and experiments in a spiral flow tester.

Thus, an ideal chemorheological procedure is one that provides good control of measurement conditions, requires a minimal sample size, measures both chemorheological properties—flow (chemoviscosity) and gel (gelation time) properties, determines basic rheological information (such as information about the linear viscoelasticity region and quantification of wall slip and yield stress), and provides chemorheological data that agree well with industrial measurements. This article examines the chemorheology of a highly filled thermoset IC encapsulant through a chemorheological procedure aimed at this ideal, using novel isothermal and nonisothermal multiwave parallel-plate rheometry.

EXPERIMENTAL

A typical highly filled thermoset IC packaging material was used in this work. The exact formulations are proprietary; however, the material is known to be an epoxy-molding compound (epoxy novolac-based) with a 70% (wt) silica filler. The samples were transported in dry ice and then placed in storage in a freezer. Samples were brought to room temperature in a desiccated environment and pressed to sample discs under a controlled environment in a sample preparation device. (The effects of sample preparation parameters on chemorheological variables were observed by a Plackett–Burman statistical experimental design, and a window of preparation parameters was chosen to minimize these effects and ensure consistent testing, as discussed in an earlier article.[14])

Kinetic data were obtained using nonisothermal DSC scans at heating rates of 2, 5, 10, 15, and 20°C/min from 25 to 250°C. The extent of the reaction, α, was assumed to be proportional to the heat generated in the reaction, similar to previous studies.[15,16]

Chemorheological testing was conducted on a Rheometrics RDSII rheometer using a parallel-plate system (diameters = 8–25 mm, gaps = 0.35–2.0 mm), enclosed by a convection oven. The oven was supplied with nitrogen for heating, from a liquid nitrogen cylinder via a small nitrogen chamber to eliminate oxidative degradation. The temperature of the sample was measured by insertion of a thermocouple inside the rheometer shaft, to within 1 mm of the bottom plate surface. Both isothermal (T = 90–120°C) and non-isothermal (dT/dt = 2–20°C/min) tests were used in both steady shear and dynamic shear modes. An outline of chemorheological tests was given in an earlier article.[14] Most tests are self-explanatory; however, the multiwave test deserves further explanation. The multiwave test superimposes a number of dynamic frequencies at specified strains into a multiple-frequency signal that is transferred to the sample. The response is measured and deconvoluted by Fourier transformations into the separate responses of the individual

Table I Kamal Model Parameters

$A1$	$E1$	$A2$	$E2$	m	n
330,000	8500	477,000	7040	1.05	1.36

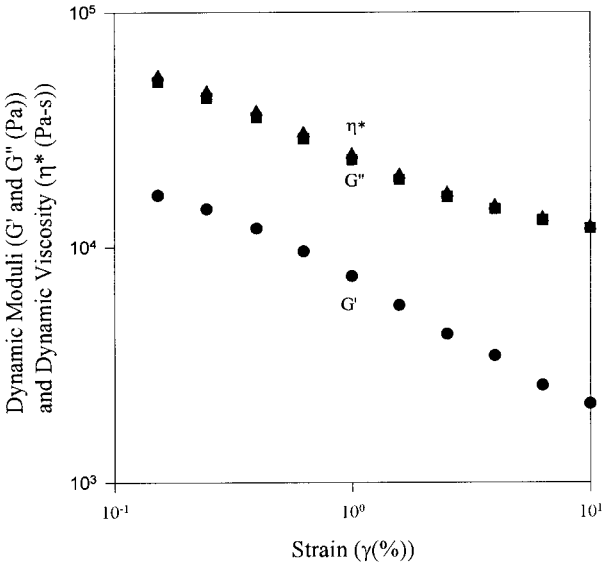

Figure 1 Strain effects on dynamic moduli and dynamic viscosity.

frequencies. The advantage of the multiwave test is that a response (e.g., viscosity) can be measured *instantaneously as a function of frequency,* and, thus, the response is not influenced by the time of testing, as in dynamic frequency sweeps.

RESULTS

Kinetic Properties

Kinetic parameters were determined from DSC nonisothermal scans. These data were fit to the Kamal model [refer to eq. (1)] by a nonlinear regression analysis:

$$\frac{d\alpha}{dt} = (k_1 + k_2\alpha^m)(1 - \alpha)^n \qquad (1)$$

where k_1 [$= A_1\exp(-E_1/T)$] and k_2 [$=A_2\exp(-E_2/T)$]are rate constants, m and n are reaction orders, and α is the conversion level. Model parameters derived from this fit are shown in Table I.

Basic Rheology

Due to the expected highly complex nature of highly filled thermoset materials, it was decided to determine the basic rheology of the material prior to extensive chemoviscosity tests. The basic rheology of highly filled systems may be defined in terms of characterizing the effects of strain, determining the presence of wall slip or yield stress, and determining the relationship between steady and dynamic viscosity.

Linear Viscoelastic Region

Dynamic strain sweep tests were undertaken to isolate the effects of strain (γ) on the dynamic viscosity (η^*) and to identify the region where the viscosity is independent of strain (linear viscoelastic region). Sample loading effects were measured and eliminated by repeat tests. Figure 1 shows the effects of strain (γ = 0.1–10%) on the

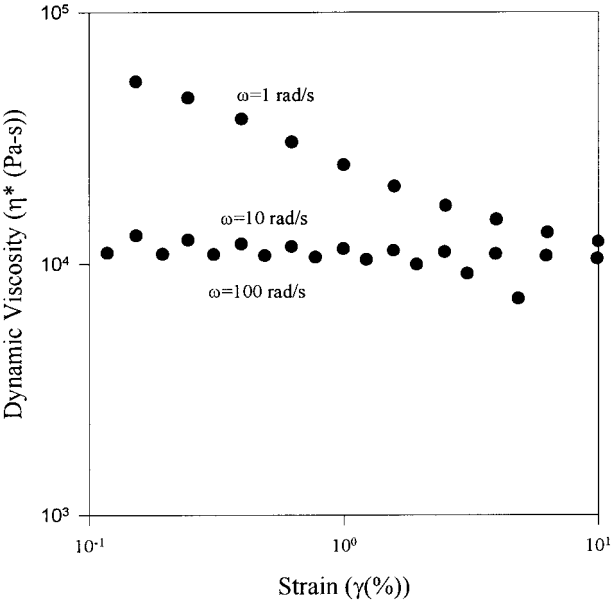

Figure 2 Strain effects on dynamic viscosity as a function of frequency.

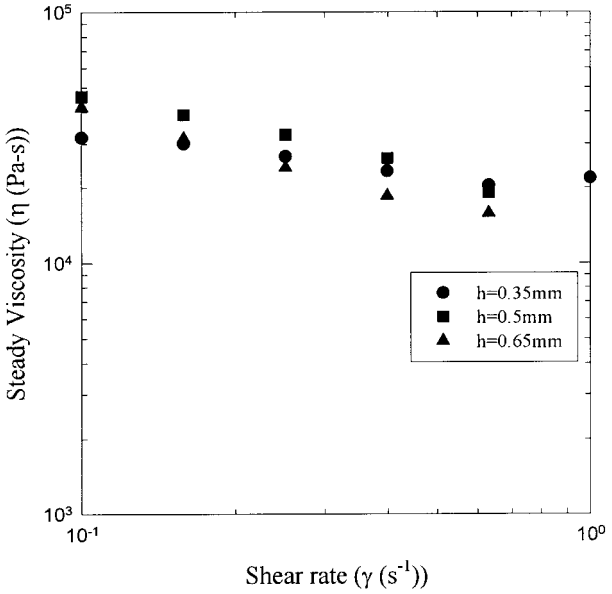

Figure 3 Effect of gap on steady viscosity profiles.

dynamic viscosity, storage modulus (G'), and loss modulus (G'') at a frequency (ω) of 1 rad/s and at a temperature (T) of 90°C. From Figure 1, it is clear there is no linear viscoelastic region for this material at the lowest possible strain tested (0.1%, due to motor limitations) and that the dynamic properties are highly strain-dependent. Strain sweep tests were also performed at higher frequencies (ω = 10, 100 rad/s) and are shown in Figure 2. This plot is unusual as higher frequencies appear to be more linear in their response than are lower frequencies, which may indicate that lower-frequency measurements are more sensitive to long-term loading effects. For future dynamic tests, we chose an arbitrary strain of 1% and assumed that for the majority of frequencies the response is linear. Note that a nonlinear response is typical of highly filled materials as noted previously by Malkin.[17] In fact, Malkin[17] expressed grave doubts to the validity of dynamic tests due to the complex nonlinear response of many highly filled materials. Future work is underway to examine the raw waveforms at low frequencies in an attempt to characterize the nonlinearity via Fourier transform analysis as outlined by Giacomin and Dealy.[18]

Slip and Yield Stress

Steady shear sweeps were undertaken to detect the presence of slip and yield stress. Slip is noted by a gap dependency of steady viscosity (viscosity decreases as gap decreases due to a greater contribution of the slip layer). If slip is present, the slip velocity may then be characterized.[19] Figure 3 shows steady shear sweeps with shear rates ($\dot{\gamma}$) from 0.1 to 1 s^{-1} at gaps (H) of 0.35–0.65 mm at a temperature of 90°C to measure the effect of the gap on the viscosity. Clearly, from Figure 3, there is no effect of the gap on the steady viscosity within the bounds of experimental variation, over the limited shear rate range tested. Temperatures were restricted by layering (lower temperatures) and cure effects (higher temperatures). The shear rates were limited by sample fracture (higher rates) and the gaps chosen were limited by unstable flows (both higher and lower gaps). Therefore, in this limited shear rate range, there was no slip evident. Future work will involve correlations of dynamic data to higher shear steady viscosity data using a capillary rheometer.

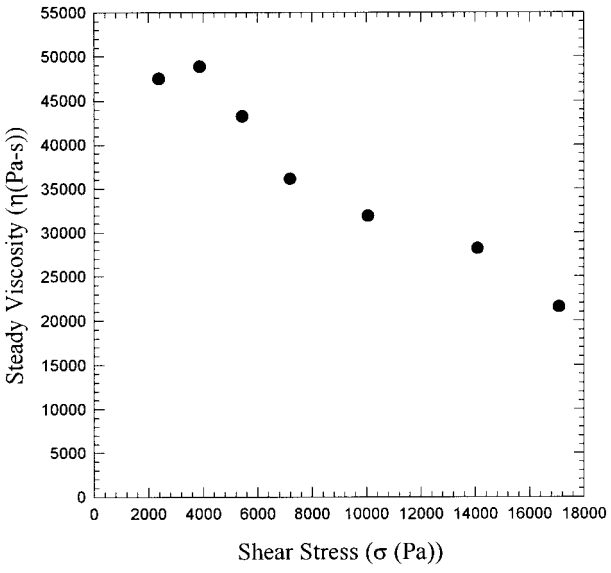

Figure 4 Yield stress determination.

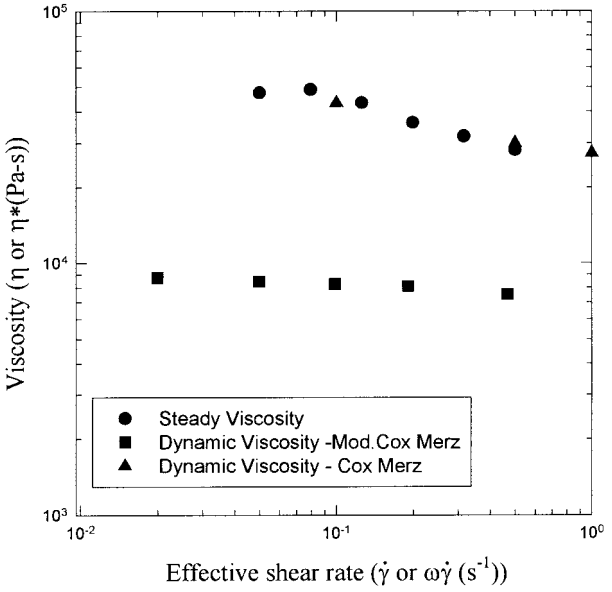

Figure 5 Comparison of Cox–Merz and modified Cox–Merz relationships.

Determination of a yield stress is made from detection of an infinite viscosity at low shear stresses (σ). Figure 4 shows a steady shear sweep ($\dot{\gamma}$ = 0.05–1 s^{-1}, H = 0.5 mm, T = 90°C) used to detect the presence of a yield stress; however, there is no evidence of an infinite viscosity at low shear stresses, and, thus, there is no detectable yield stress. This result was confirmed by the nonexistence of a residual stress after steady relaxation tests.

Steady Viscosity–Dynamic Viscosity Relationship

To utilize the parallel-plate rheometer system for the evaluation of chemoviscosities at realistic shear rates, dynamic shear tests must be used. In

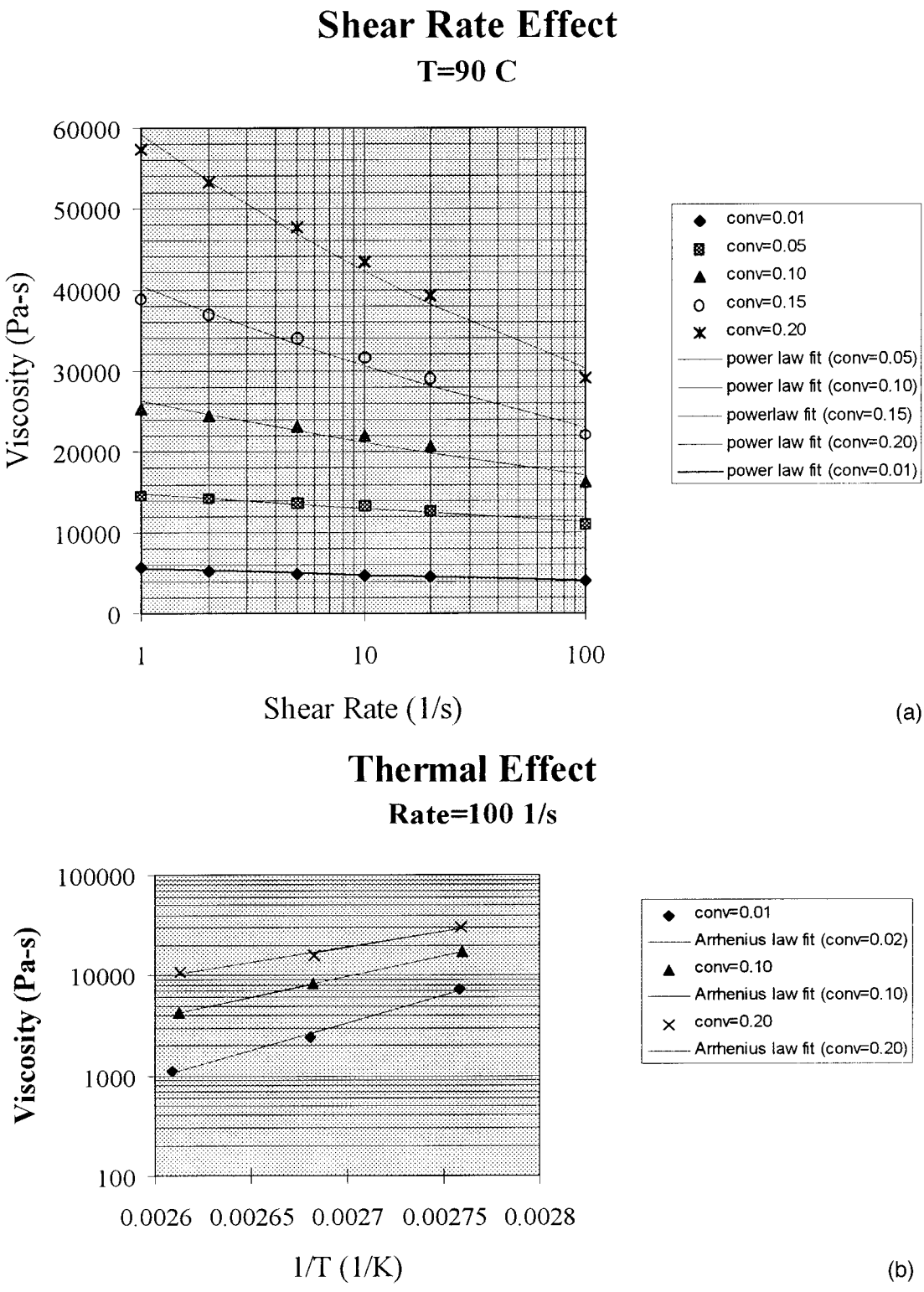

Figure 6 Effects of (a) shear rate, (b) temperature, and (c) cure level on isothermal chemoviscosity as characterized by the power Law model.

the parallel-plate system, steady shear rates are restricted for high-viscosity materials due to sample fracture. Therefore, a correlation must be made between the dynamic shear viscosity and the steady shear viscosity to achieve high rate measurements. A comparison of steady shear vis-

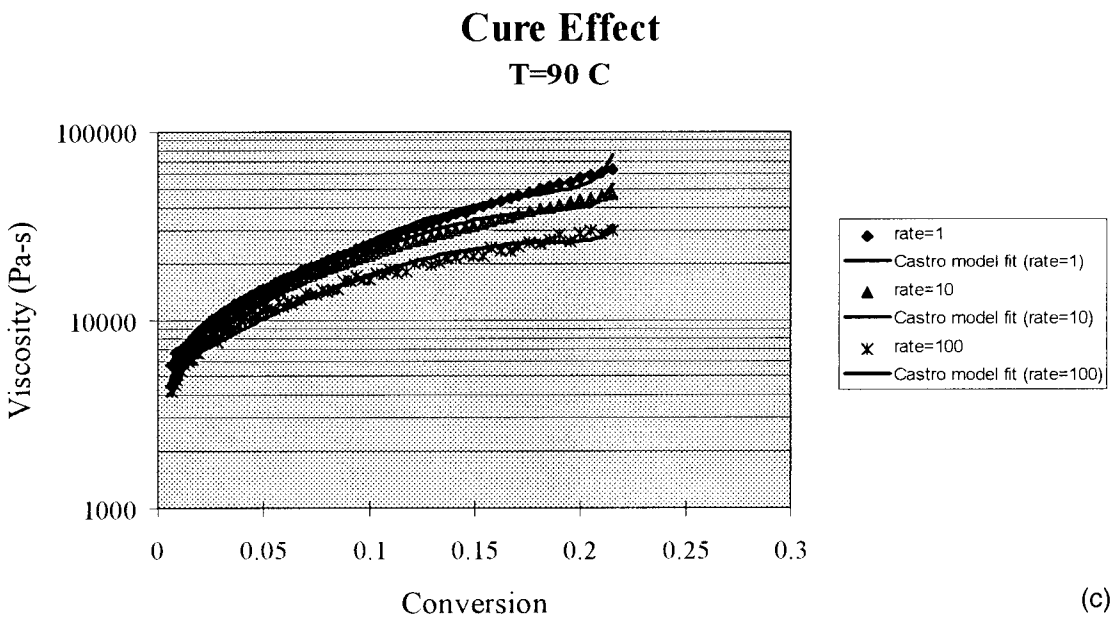

Figure 6 (*Continued from the previous page*)

cosity and dynamic shear viscosity is made by comparing the responses from a steady shear sweep and a multiwave time test.

Empirical correlations exist to relate the steady viscosity to the dynamic viscosity. The Cox–Merz rule states that the steady viscosity is equal to the dynamic viscosity at equivalent shear rates or frequencies, i.e.,

$$\eta(\dot{\gamma}) = \eta^*(\omega) \tag{2}$$

This rule has been shown to hold for many materials including filled epoxy resin systems.[5] Also, a modified Cox–Merz relationship was developed recently[3] for highly filled materials, which states that the steady viscosity is equal to the dynamic viscosity at equivalent *effective shear rates.* The effective shear rates are $(\dot{\gamma})$ for steady shear and $(\gamma\omega)$ for dynamic shear. Symbolically, this may be represented as

$$\eta(\dot{\gamma}) = \eta^*(\gamma\omega) \tag{3}$$

A comparison of steady shear and dynamic shear viscosities using the Cox–Merz and the modified Cox–Merz correlations are shown in Figure 5 using a steady shear sweep ($\dot{\gamma}$ = 0.05–1 s^{-1}, T = 90°C) and isothermal multiwave time tests (ω = 0.1–1 [Cox–Merz] or 1–100 rad/s [modified Cox–Merz], γ = 1%, T = 90°C). Clearly, the Cox–Merz relationship correlates the steady and dynamic data much better than does the modified Cox–Merz relationship. It must be noted, however, that the dynamic data was obtained at a strain of 1%. Thus, basic rheological tests found that the dynamic response was in the linear viscoelastic region (for the majority of frequencies), there was no wall slip or yield stress, and the Cox–Merz relationship could be used to correlate dynamic viscosities to steady shear viscosities.

Chemoviscosity Tests

Isothermal Chemoviscosity

Isothermal chemoviscosity tests were used to examine shear rate $(\dot{\gamma})$, thermal (T), and conversion (α) effects on the chemoviscosity. These individual effects may be examined in isolation by fits to individual models [shear rate: $\eta_{sr} = \eta_{sr}(\dot{\gamma})$; thermal: $\eta_T = \eta_T(T)$; and conversion: $\eta_c = \eta_c(\alpha)$] and then combined into an overall model [$\eta_I(\gamma, T, \alpha)$]. Isothermal chemoviscosity tests were conducted using isothermal multiwave tests (ω = 1–100 rad/s, γ = 1%, T = 90, 100, and 110°C).

Shear-rate Effects. The shear-rate effects on chemoviscosity have been described by the power law model, given in the following equation, for fixed temperatures (T = 90, 100, and 110°C) and levels of conversion (α = 0.00–0.20):

$$\eta_{sr}(\dot{\gamma})_{T,\alpha} = A\dot{\gamma}^b \tag{4}$$

where A is the power law constant and b is the power law coefficient.

Table II Power Law Model (Shear Effects), Arrhenius Model (Temperature Effects), and Castro Model (Cure Effects) Parameters from Fit to Isothermal Data

Shear Rate Effect Conditions	A	B
T = 90°C		
a = 0.00	5600	−0.07
a = 0.05	14,800	−0.06
a = 0.10	26,300	−0.10
a = 0.15	40,400	−0.12
a = 0.20	59,200	−0.15
T = 100		
a = 0.02	3200	−0.13
a = 0.10	11,000	−0.08
a = 0.20	32,500	−0.15
T = 110		
a = 0.02	3600	−0.29
a = 0.10	10,100	−0.19
a = 0.20	50,500	−0.35

Temperature Effects	C	D
w = 1 rad/s		
a = 0.05	1.37*e*-05	7360
a = 0.10	3.05*e*-06	8040
a = 0.15	1.46*e*-04	6830
a = 0.20	1.79*e*-04	7215
w = 10 rad/s		
a = 0.02	1.54*e*-09	10,600
a = 0.10	1.51*e*-07	9300
a = 0.20	1.10*e*-02	5500
w = 100 rad/s		
a = 0.02	5.94*e*-12	12,600
a = 0.10	7.25*e*-08	9500
a = 0.20	8.13*e*-05	7100

Cure Effect Conditions	E	F	G
T = 90°C			
w = 1	6000	4.0	−15.5
w = 10	5400	3.9	−15.5
w = 100	5000	3.4	−13.6
T = 100°C			
w = 1	2400	3.9	−14.5
w = 10	1900	4.3	−16.4
w = 100	1700	4.0	−15.6
T = 110°C			
w = 1	2200	3.5	−11.0
w = 10	940	4.7	−17.0
w = 100	700	4.6	−17.5

A typical power law model fit is shown in Figure 6(a) for T = 90°C and (α = 0.00–0.20) and model parameters for all conditions are displayed in Table II. From Figure 6(a), it is evident that the power law model describes the shear-rate effects quite well, and this is typical of other conditions. The power law factor increases with cure level and decreases with temperature as expected. The power law coefficient remains reasonably constant with temperature and conversion, which is similar to previous literature.[20]

Thermal Effects. The effects of temperature on the chemoviscosity has been fit to the Arrhenius model, given in the following equation, for fixed frequencies (ω = 1, 10, and 100 rad/s) and levels of conversion (α = 0.00–0.20):

$$\eta_T(T)_{\omega,\alpha} = C \exp(D/T) \qquad (5)$$

where C is the preexponential factor and D is the activation temperature.

A typical Arrhenius model fit is shown in Figure 6(b) for ω = 100 rad/s and (α = 0.00–0.20) and model parameters for all conditions are displayed in Table II. From this fit, it is evident that the Arrhenius law model describes the thermal effects quite well, and this is typical of all conditions. The preexponential factor increases with cure level and decreases with shear rate as expected. The activation temperature remains reasonably constant with shear rate and conversion, which agrees with other findings.[20] The average activation energy ($\Delta E = D \times R$, where R = universal gas constant) is 77.6 kJ/mol, which is in good agreement with the value of 78.5 kJ/mol obtained by Ryan and Kamal[20] for their highly filled IC packaging resin.

Conversion Effects. The effects of conversion on the chemoviscosity has been described by the Castro model,[21] given in the following equation, for fixed temperatures (T = 90, 100, and 110°C) and frequencies (ω = 1, 10, and 100 rad/s):

$$\eta_c(\alpha)_{T,\omega} = E[\alpha_{\text{gel}}/(\alpha_{\text{gel}} - \alpha)]^{(F+G\alpha)} \qquad (6)$$

Table III Overall Macosko Model Parameters from Isothermal Data and Nonisothermal Data

Isothermal Parameters–Macosko Model				
A_I (Pa-s)	B_I	C_I (K)	D_I	E_I
2.20*e*-05	−0.13	7040	3.9	−14.7
Nonisothermal Parameters–Macosko Model				
A_{NI} (Pa-s)	B_{NI}	C_{NI} (K)	D_{NI}	E_{NI}
8.76*e*-20	−0.13	19,200	6.8	−27.1

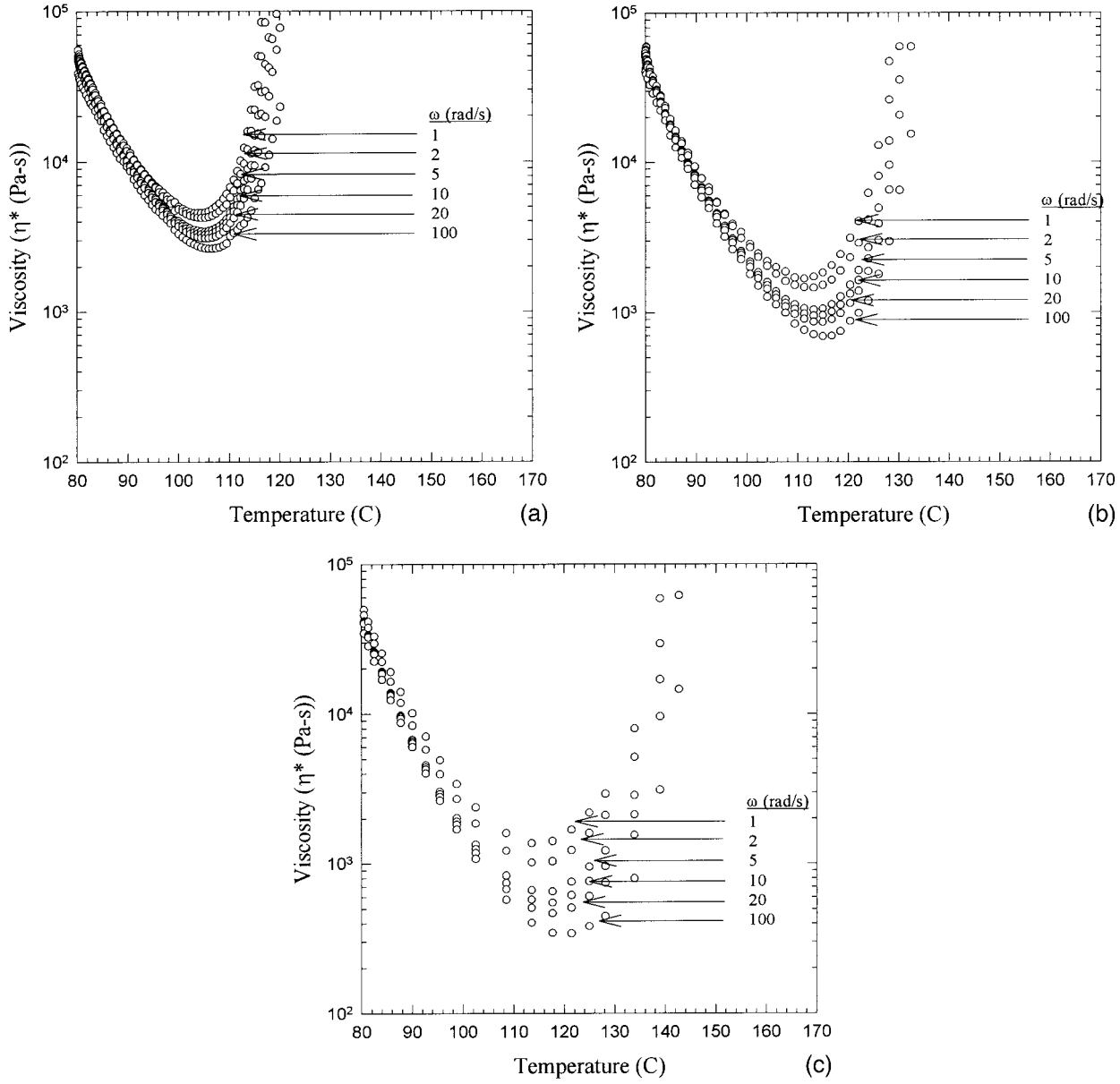

Figure 7 Shear and cure effects on nonisothermal chemoviscosity at (a) dT/dt = 2°C/min, (b) 5°C/min, and (c) 10°C/min.

where E, F, and G are constants and α_{gel} is the conversion at the gel point (=0.22).

A typical Castro model fit is shown in Figure 6(c) for T = 90°C and (ω = 1, 10, and 100 rad/s) and model parameters for all conditions are displayed in Table II. From this fit, it is evident that the Castro model describes the cure effects quite well, and this is typical of all conditions. The initial factor (E) decreases with temperature and shear rate as expected. The other coefficients show some variation with temperature and shear rate.

Overall Effects. An overall model for all isothermal data may be then represented by a combination of the power law, Arrhenius law, and Castro model, also known as the Macosko model, and as shown by the following equation:

$$\eta(\dot{\gamma}, T, \alpha) = A_I(\dot{\gamma})^{b_I} \exp(C_I/T) \times [\alpha_{gel}/(\alpha_{gel} - \alpha)]^{(D_I + E_I\alpha)} \quad (7)$$

where A_I, B_I, C_I, D_I, and E_I can be calculated from the individual effects data. Overall model parameters are shown in Table III. The Macosko model fit was quite good to all isothermal data.

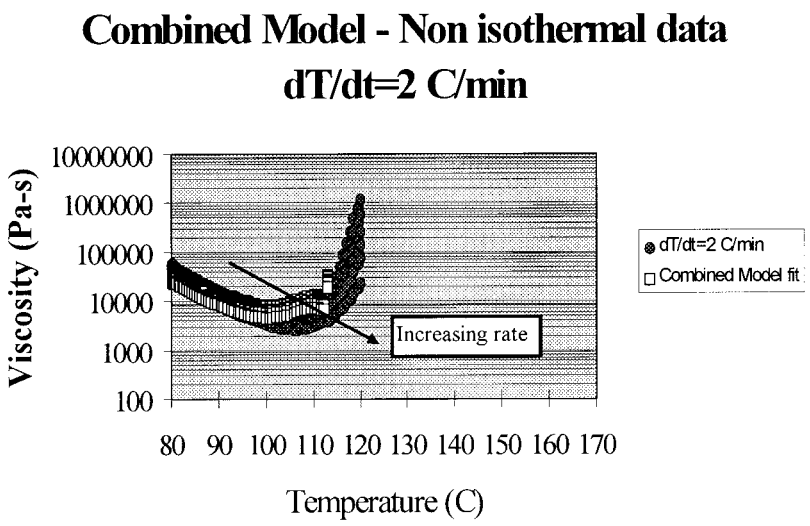

Figure 8 Fit of Macosko model to nonisothermal data.

Nonisothermal Chemoviscosity

The advantages of nonisothermal testing over isothermal tests are that the temperature profiles are more like processing conditions, higher temperatures can be achieved, and processing information such as optimal heating rate and optimal minimum viscosity can be measured. Nonisothermal chemoviscosity tests were conducted using nonisothermal multiwave tests (ω = 1–100 rad/s, γ = 1%, dT/dt = 2, 5, and 10°C/min and T = 80–170). The results of the tests may be examined in Figure 7. From Figure 7, it can be seen that a higher heating rate extends the minimum viscosity to lower values at higher temperatures, indicating that cure effects are initially overwhelmed by thermal effects at higher heating rates. Also, higher heating rates cause a wider minimum viscosity plateau, as reported in the literature.[22] Optimal heating rates and minimum viscosities may be determined from Figure 7 depending on process requirements.

Nonlinear regression of the Macosko model [refer to eq. (8)] to the nonisothermal data at all heating rates (dT/dt = 2, 5, and 10°C/min) was undertaken and the fit is shown in Figure 8 for a heating rate of 2°C/min. The model parameters from the fit to all data are shown in Table III:

$$\eta(\dot{\gamma}, T, \alpha) = A_{\mathrm{NI}}(\dot{\gamma})^{b_{\mathrm{NI}}} \exp(C_{\mathrm{NI}}/T) \times [\alpha_{\mathrm{gel}}/(\alpha_{\mathrm{gel}} - \alpha)]^{(D_{\mathrm{NI}}+E_{\mathrm{NI}}\alpha)} \quad (8)$$

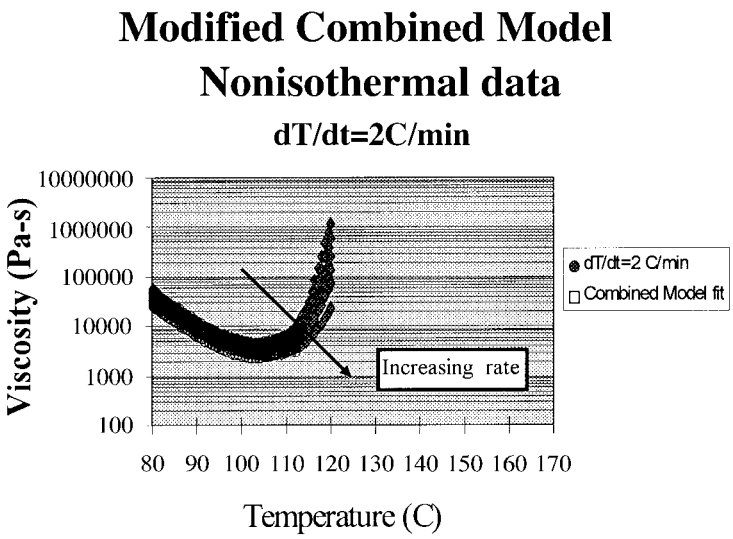

Figure 9 Fit of modified-Macosko model to nonisothermal data.

Table IV Modified-Macosko Model Parameters from Fit to Nonisothermal Data

A (Pa-s)	B	C (K)	D_0	D_1 (1/K)	E_0	E_1 (1/K)
8.76*e*-20	−0.13	19,200	−82	253	0.23	−0.71

From the data, it can be seen that the fit is reasonable up to the gel point and this is typical for all heating rates. However, when individual fits of the Macosko model at each heating rate were examined, they showed better fits than did the overall fit to all the data. The improved fit was thought to be due to the effects of temperature on parameters D and E. A model that has been investigated, which allows for temperature effects on parameters D and E, is the modified Macosko model[11] as shown in eq. (9). A noticeable improvement in fits were found using this model, and a typical fit is shown in Figure 9 for a heating rate of 2°C/min. Model parameters are shown in Table IV:

$$\eta(\dot\gamma, T, \alpha) = A(\dot\gamma)^b \exp(C/T) \times [\alpha_{\text{gel}}/(\alpha_{\text{gel}} - \alpha)]^{(D^* + E^*\alpha)}$$

where

$$D^* = D_0 + D_1 \times T$$
$$E^* = E_0 + E_1 \times T \qquad (9)$$

(Although not shown, it is important to note that the overall model parameters *calculated* [by determination of parameters *AI* to *EI* from individual-effect isothermal shear rate, thermal, and conversion data] also predicted nonisothermal data well, with the exception of over estimating viscosities at temperatures below 90°C [the lowest isothermal temperatures used].)

Gel Point Data

The gel point of the highly filled thermoset material was determined by the independence of the loss tangent on frequency, as previously discussed in the literature.[1] The tests that were used were isothermal multiwave tests (ω = 1, 2, and 5 rad/s, γ = 1%, T = 90, 100, 110, and 120°C) and the gel points are shown in Table V and Figure 10. From these results, it is clear that the gel times decrease with temperature as expected. Also, the gel times are predicted by an Arrhenius model which is given by the following equation:

$$t\text{gel} = A \exp(E/T) \qquad (10)$$

where $A = 3.62 \times 10^{-6}$ s and E = 7360 K. This relationship is also in excellent agreement with the gel time given in the specification sheet for the material ($t$gel = 25 s at 180°C). Note also that the values of the loss tangent do not equal 1 at the gel point, which has been reported by others.[23]

The gel conversion level was determined from the above data and kinetic data and is around 0.22–0.35. This variation is due to the errors in gel time measurements.

Other tests were conducted to measure the gel point including the crossover of the G' and G'' method (dynamic time test: ω = 1 rad/s, γ = 1%, T = 100°C), the inflection in the G'' method (dy-

Table V Gelation Times from Independence of Loss Tangent Method

Temperature (°C)	t gel (s)	Tan δ at Gel
90	2300 ± 100 s	3.2
100	1100 ± 100 s	3.0
110	650 ± 100 s	2.5
120	500 ± 100 s	1.0

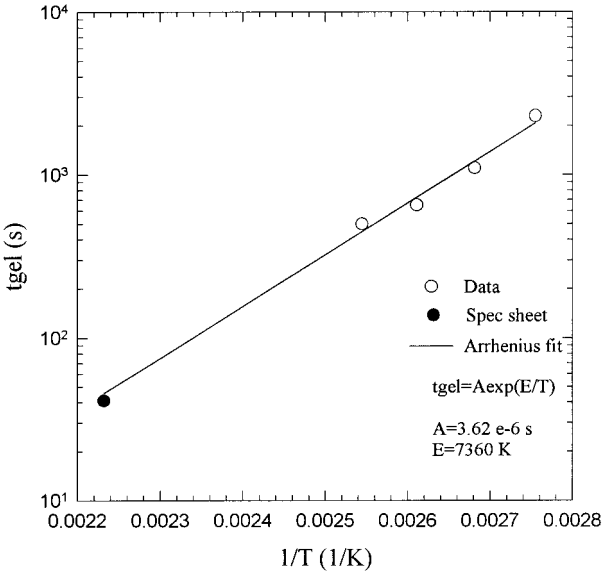

Figure 10 Gel times as a function of temperature.

namic time test: $\omega = 1$ rad/s, $\gamma = 1\%$, $T = 100°C$), and the attainment of infinite steady viscosity (steady time test $\gamma = 0.05$ s $- 1$, $T = 100°C$). A summary of gel times from these tests, and the independence of the loss tangent on the frequency test, is shown in Table VI. From these results, it can be concluded there is no statistical difference in gel times measured by either technique within experimental errors, although recent literature[24] indicates that there may be variations in gel times when using methods other than the independence of the loss tangent on the frequency test.

Verification Tests

The above nonisothermal chemorheological data was tested in a TSET (Moldflow Pty Ltd) simulation as an introductory verification test. A rectangular plaque ($40 \times 10 \times 2$ mm) was used in both filling and curing analyses. The following input parameters were used[2]:

Maximum injection pressure = 7 MPa
Maximum clamp tonnage = 220 tonnes
Mold temperature = 175°C
Melt temperature = 90°C
Injection time = 15 s

These material data were compared to typical industrial data.[2] The results from the filling and curing analysis are summarized in Table VII, with output variables such as pressure and temperature in the mold, maximum shear stresses and shear rates, and calculated ejection time at 60% cure. These results indicate that the chemorheological data produce results in excellent agreement with typical industrial data.

CONCLUSIONS AND FUTURE WORK

The main conclusions from this work were as follows:

Table VI Comparison of Gelation Times from Various Rheological Methods at 100°C

Method	t gel (s)
Loss tangent	1100 ± 100 s
Crossover of G' and G''	1300 ± 100 s
Inflection in G''	1000 ± 100 s
Infinite viscosity	1000 ± 100 s

Table VII Comparison of Filling and Curing Results from Simulation with Current and Typical Industrial Data[2]

Property	Current	Typical
Maximum pressure	4 kPa	1–5 kPa
Temperature profile	89–95°C	90–95°C
Maximum stress	1 kPa	0–1 kPa
Maximum shear rate	34 1/s	20–40 1/s
Ejection time (at 60% cure)	70 s	60–80 s

- Chemorheological data were obtained by isothermal (instructive) and nonisothermal (realistic) tests on a parallel-plate rheometer using steady and dynamic multiwave tests.
- Viscosity data was linear (for most frequencies) with respect to strain, showed no slip or yield stress, and was predicted by the Cox–Merz relationship.
- The Macosko model fit the chemorheological data reasonably; however, the modified Macosko model improved the fit.
- The gel times, measured by the independence of the loss tangent on frequency method, were fitted by an Arrhenius model and agreed well with supplier's specification data.
- The TSET analysis showed that the data was realistic.

Future work will include

- Analysis of the nonlinear effects of strain at low frequencies on chemoviscosity.
- Determination of high shear rate viscosities.
- Use of the data in more industrial applicable simulation models.

I would like to acknowledge Dr. Michael Mackay and Dr. Chris Friedl (Moldflow) and for their comments during experimental work. Also, thanks to Professor Erdogan Kiran for an invitation to present this work at the Thermoset Symposium at Princeton. Appreciation also goes to Moldflow and The University of Queensland for funding this work.

REFERENCES

1. L. T. Nguyen, A. Danker, N. Santhiran, and C. R. Shervin, in *Proceedings from ASME Winter Annual Meeting,* Nov. 8–13, 1992.

2. L. T. Nguyen, in *Proceedings from 43rd IEEE Electronic Components and Technology Conference,* June 1–3, 1993.
3. P. Doriswamy, A. N. Mujumdar, I. Tsao, A. N. Beris, S. C. Danforth, and A. B. Metzner, *J. Rheol.,* **35,** 647 (1991).
4. G. W. M. Peters, A. B. Spoelestra, M. H. H. Meuwissen, R. Corbey, and H. E. H. Meijer, in *Topics in Applied Mechanics,* J. F. Dijksman and F. T. M. Nieuwstadt, Eds., Kluwer, Amsterdam, The Netherlands, 1993, p. 331.
5. M. H. Pahl and D. Hesenkamp, *Rheology,* **93,** 97 (1993).
6. W. P. Cox and E. H. Merz, *J. Polym. Sci.,* **28,** 619 (1958).
7. P. J. Halley, M. E. Mackay, and G. E. George, *High Perform. Polym.,* **6,** 405 (1994).
8. E. E. Holly, S. K. Venkataraman, F. Chambon, and H. H. Winter, *J. Non-Newt. Fluid Mech.,* **27,** 17 (1988).
9. H. Ng and I. Manas-Zloczower, *Polym. Eng. Sci.,* **33**(4), 211 (1993).
10. L. L. Blyler, H. E. Bair, P. Hubbauer, S. Matsuoka, D. S. Pearson, G. W. Poelzing, R. C. Progelhof, and W. G. Thierfelder, *Polym. Eng. Sci.,* **26**(20), 1399 (1986).
11. S. Han and K. K. Wang, *Proceed. ANTEC'94,* 935 (1994).
12. L. T. Manzione and J. D. Weld, *Proceed. ANTEC'94,* 1371 (1994).
13. U. F. Gonzalez, S. F. Shen, and C. Cohen, *Polym. Eng. Sci.,* **32**(3), 172 (1992).
14. P. J. Halley and M. E. Mackay, *Proceed. ANTEC'95,* 879 (1995).
15. H. Ng and I. Manas-Zloczower, *Polym. Eng. Sci.,* **29,** 1097 (1989).
16. T. H. Hsieh and A. C. Su, *J. Appl. Polym. Sci.,* **44,** 165 (1992).
17. A. Y. Malkin, *Adv. Polym. Sci.,* **96,** 70 (1990).
18. A. J. Giacomin and J. M. Dealy, in *Techniques in Rheological Measurements,* A. Collyer, Ed., Chapman and Hall, London, 1993, p. 99.
19. A. Yoshimura and R. K. Prud'homme, *J. Rheol.,* **32,** 53 (1988).
20. M. E. Ryan and M. R. Kamal, in *Proceedings of the VIIth International Congress on Rheology,* 1976, p. 290.
21. J. M. Castro and C. W. Macosko, *Polym. Eng. Sci.,* **28,** 250 (1982).
22. *Understanding Rheological Testing,* Rheometrics Brochure, 1990.
23. L. Matejka, *Polym. Bull.,* **26,** 109 (1991).
24. L. Boutin, A. Ajji, and L. Choplin, in *Proceedings XIth International Congress on Rheology,* Brussels, Belgium, 1992.